

Appendix A: Observations

The observations were obtained with compact and extended array configurations, with baselines in the range $\sim 12 - 300$ m and $\sim 30 - 2000$ m, respectively. The field of view (FoV) of the 12m ALMA antennas ranges from $\sim 69''$ at 84 GHz to $\sim 50''$ at 115.5 GHz. Additional observations were performed with the IRAM 30m telescope to recover the flux filtered out by the interferometer. Observations were centered on the position of the star, with coordinates J2000.0 R.A.= $09^{\text{h}}47^{\text{m}}57^{\text{s}}.446$ and Dec.= $13^{\circ}16'43''.86$, according to the position of the $\lambda 1$ mm continuum emission peak (Cernicharo et al. 2013). A detailed description of the spectral survey will be presented elsewhere (Cernicharo et al., in prep). The data were calibrated using the CASA¹ software package, and imaged and cleaned with GILDAS² software package. We used the SDI cleaning algorithm since HOGBOM could generate artificially clumpy structures for high spatial resolution observations.

For the emission lines studied here, data from the ALMA compact and extended configurations were merged, after continuum subtraction, with the short-spacing data obtained with the IRAM 30m telescope. In particular, since the NaCN emission is relatively weak, we present low spatial resolution NaCN maps with high S/N, obtained by merging the ALMA compact configuration and short-spacing data, and high spatial resolution maps with low S/N, obtained when merging both ALMA configurations plus the short-spacing data (see Table 1 for details). In order to increase the S/N, we stacked the NaCN emission of the different lines lying at 3 mm. These maps are presented in Figs.A.1 and A.2.

We also present a map of MgNC $8_{17/2} - 7_{15/2}$, observed at the same time as the 3 mm ALMA line survey. As for NaCN emission map, we merged single-dish OTF data with those of the extended and compact ALMA configurations. This map is presented in Fig. A.3

In addition, we recently obtained ALMA Cycle-4 data that cover two NaCN transitions at $\lambda 2$ mm (see Table 1). These observations consisted in a mosaic of seven fields covering a FOV of $\sim 214''$. We note that for these transitions we did not have short-spacing data, and thus the maps only rely on ALMA visibilities. Although the NaCN emission is relatively compact, some flux is expected to be filtered out. The baselines of the interferometer were in the range $\sim 12 - 408$ m. For a detailed description of these ALMA-Cycle 4 observations see Velilla Prieto et al. (in prep). These maps are shown in Figs. A.4 and A.5.

¹ <http://casa.nrao.edu/>

² <http://www.iram.fr/IRAMFR/GILDAS/>

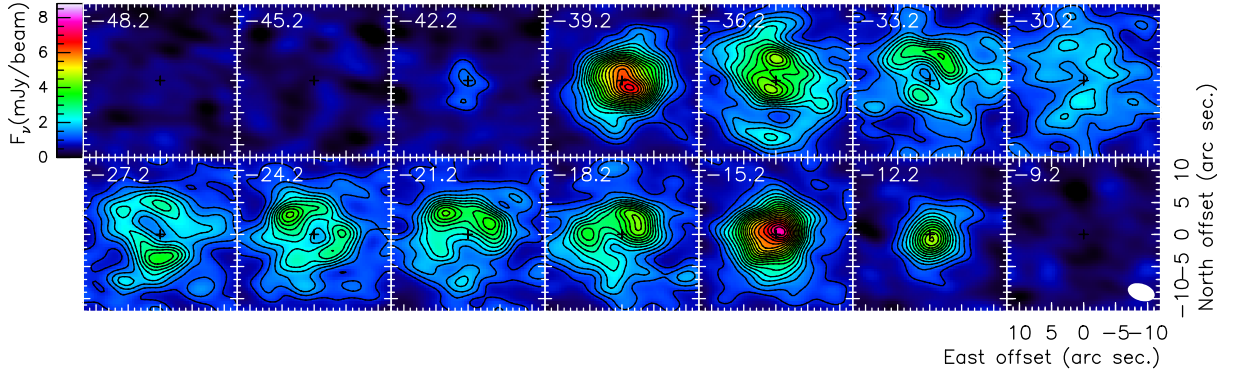


Fig. A.1: Low spatial resolution interferometric map of the NaCN stacked emission of the transitions at λ 3 mm presented in Table 1. In the upper left corner of each panel we note the v_{LSR} of the channel ($V_{sys} = -26.5 \text{ km s}^{-1}$). The lowest contour corresponds to a value of 3σ , and the rest of the contours are equally spaced in jumps of 2σ with respect to the first contour. The rms of the map is $\sigma = 0.8 \text{ mJy beam}^{-1}$. The beam size is drawn in the last panel. The HPBW is $4''.3 \times 2''.6$ with a P.A. of 72° .

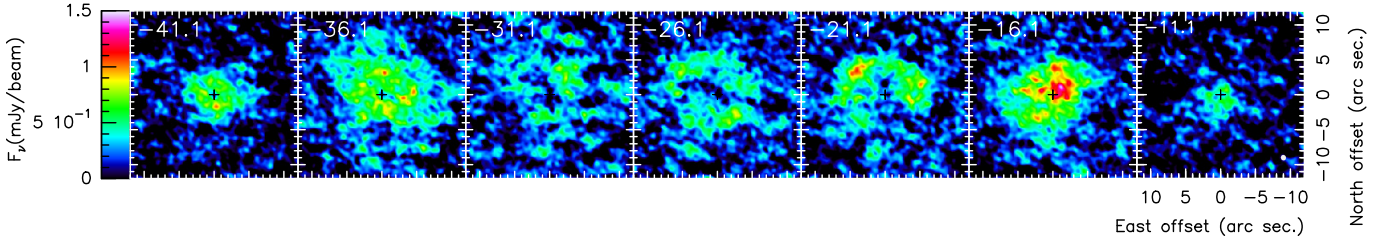


Fig. A.2: High spatial resolution interferometric map of the NaCN stacked emission of the transitions presented in Table 1. In the upper left corner of each panel we note the v_{LSR} of the channel ($V_{sys} = -26.5 \text{ km s}^{-1}$). The rms of the map is $\sigma = 0.76 \text{ mJy beam}^{-1}$. The beam size is drawn in the last panel. The HPBW is $0''.8 \times 0''.7$ with a P.A. of 20° . The flux density scale is in Jy beam^{-1} .

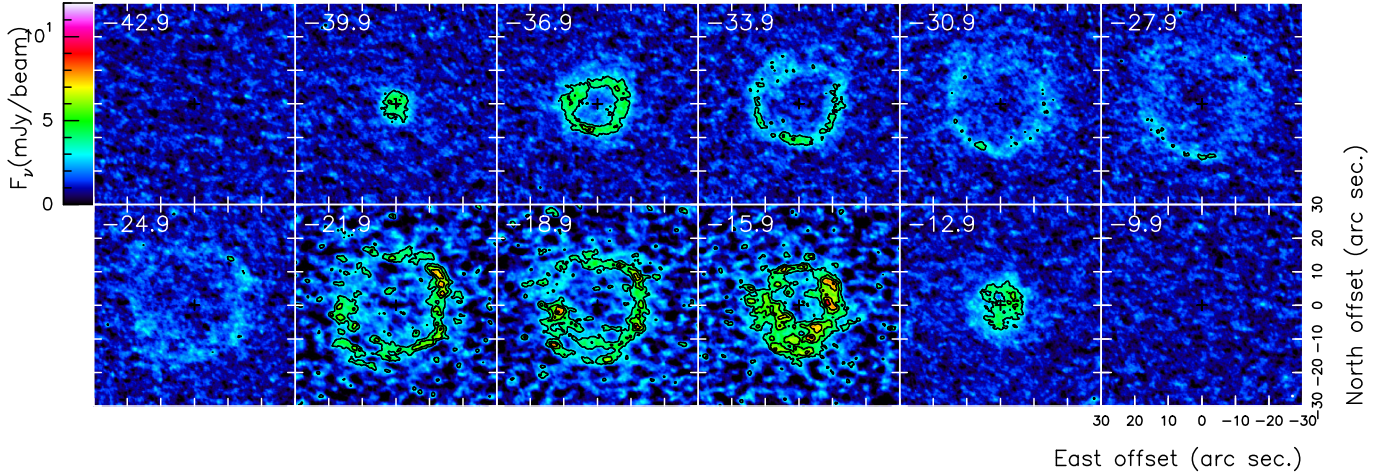


Fig. A.3: Interferometric map of the MgNC $8_{17/2} - 7_{15/2}$ emission of the transitions observed within ALMA project 2013.1.00432.S. In the upper left corner of each panel we note the v_{LSR} of the channel ($V_{sys} = -26.5 \text{ km s}^{-1}$). The lowest contour corresponds to a value of 3σ , and the rest of contours are equally spaced in jumps of 2σ with respect to the first contour. The rms of the map is $\sigma = 0.9 \text{ mJy beam}^{-1}$. The beam size is downgraded to that of Fig. A.1 and is drawn in the last panel. The HPBW is $0''.9 \times 0''.8$ with a P.A. of 33° . The flux density scale is in mJy beam^{-1} .

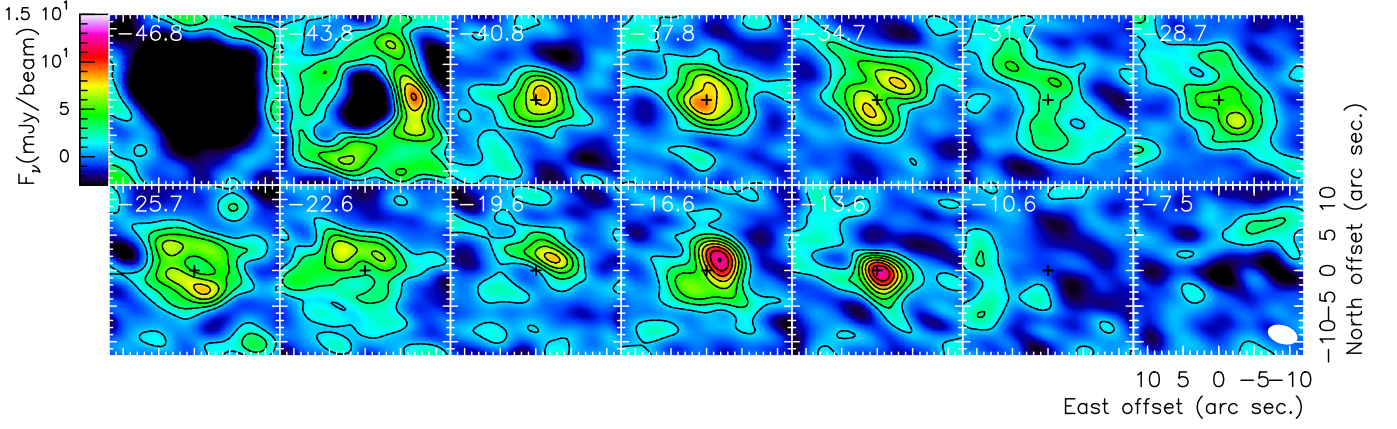


Fig. A.4: λ 2 mm interferometric map of the NaCN $9_{1,8}-8_{1,7}$ emission. The emission of the line C_3H_2 $3_{1,2}-2_{2,1}$ at 145089.61104 MHz is partially blended with that of NaCN and can be seen in the first channels. The central channels of the NaCN are, however, free of this pollution. In the upper left corner of each panel we note the v_{LSR} of the channel ($V_{sys} = -26.5 \text{ km s}^{-1}$). The lowest contour corresponds to a value of 1σ , and the rest of contours are equally spaced in jumps of 1.5σ with respect to the first contour. The rms of the map is $\sigma = 1.1 \text{ mJy beam}^{-1}$. The beam size is downgraded to that of Fig. A.1 and is drawn in the last panel. The HPBW is $0''.8 \times 0''.7$ with a P.A. of 20° . The flux density scale is in Jy beam^{-1} .

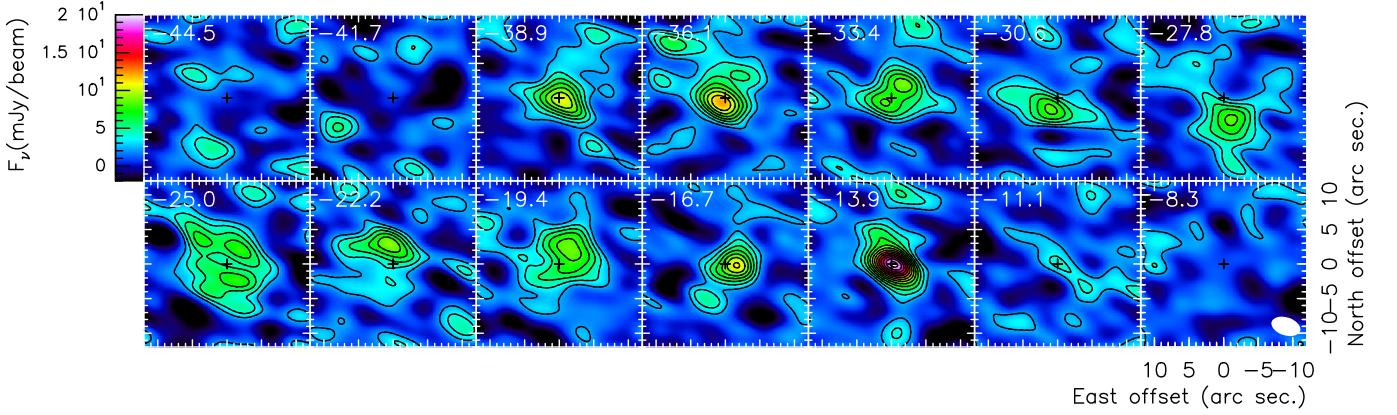


Fig. A.5: λ 2 mm interferometric map of the NaCN $10_{2,8}-9_{2,7}$ emission of the transitions presented in Table 1. In the upper left corner of each panel we note the v_{LSR} of the channel ($V_{sys} = -26.5 \text{ km s}^{-1}$). The lowest contour corresponds to a value of 1σ and the rest of contours are equally spaced in jumps of 1σ with respect to the first contour. The rms of the map is $\sigma = 1.5 \text{ mJy beam}^{-1}$. The beam size is downgraded to that of Fig. A.1 and is drawn in the last panel. The HPBW is $0''.8 \times 0''.7$ with a P.A. of 20° . The flux density scale is in Jy beam^{-1} .